Atmos. Chem. Phys. Discuss., 11, C4810–C4821, 2011
www.atmos-chem-phys-discuss.net/11/C4810/2011/

Atmospheric Chemistry and Physics Discussions

Interactive comment on "Measurements of gaseous H_2SO_4 by AP-ID-CIMS during CAREBeijing 2008 Campaign" *by* J. Zheng et al.

J. Zheng et al.

minhu@pku.edu.cn

Received and published: 11 June 2011

We are grateful to Reviewer #1 for the helpful suggestions. The manuscript has been revised accordingly. Please note that a new figure is inserted before the original Fig. 5, which now is referred as the Fig. 6. In addition, a new panel of sulfate to SO2 ratio is added to Fig. 6 as Fig. 6c. All figure numbers in this response refer to the numbers in the discussion paper.

1) p. 5024, lines 5-11. I would like to see more discussion of the calibration methodology. Was the apparatus described by Zheng et al. (Anal. Chem., 2010) used? If so, would you please summarize in 2-3 sentences the methodology?

Response: Yes, the apparatus used for calibrations was the same as the one described

by Zheng et al. (2010). We have inserted the following paragraph into the manuscript (Section 2.1) to summarize the calibration methodology. The calibration device was a 0.5-in OD UV point light source, consisting of a mercury lamp (UVP, 90-0012-01), a bandpass filter centered at 185 $\pm$ 25 nm (OMEGA Optical, XB32), and a set of turbulence-inducing fins. During calibration, H2O molecules in the ambient air were photolyzed by the 184.9 nm radiations into OH radicals, which were converted into GSA (shown as R1-R3) by excess SO2 (Sigma-Aldrich) supplied in the front of the inlet. The formed GSA concentrations were determined by the H2O concentration and the 184.9 nm radiation intensity. The H2O concentration was determined by the ambient temperature and relative humidity obtained from the meteorological station measurements. The 184.9 nm radiation intensity was measured by a CsI phototube (Hamamatsu R5764) certified by the National Institute of Standards and Technology (NIST). Since the 184.9 nm radiation attenuated significantly in the air, a set of fins were used to evenly distribute the formed GSA inside the inlet. A series of orifices with diameters ranging from 0 to 5 mm were used to vary the light source intensity and the formed GSA concentration.

2) p. 5025, line 12. The SO2 analyzer is probably an Ecotech EC9850 model;

Response: The SO2 analyzer is an Ecotech EC9850. The manuscript has been revised accordingly.

3) p. 5025, line 13. Was there measurement of NO2? If not, how was Eqn. 3, in which OH is calculated, solved? Was O3 measured at the site?;

Response: Yes, there were both O3 (Thermo Scientific, Model 49C) and NO2 (Thermo Scientific, Model 42C) measurements at the site. The descriptions of both instruments have been inserted into the section 2.2.

4) p. 5026, lines 13-20. I am puzzled by the discussion of diffusion and turbulence here and also in the Zheng et al. (2010) paper. If the flow is laminar, wall losses by molecular diffusion will not be a function of tube diameter, since for a given flowrate the

residence time will increase proportionally to the diffusion time if diameter is changed. However, the flow here is surely turbulent, with Reynolds numbers exceeding 16 000. Thus a spiral flow mixer for calibration (Zheng et al.) is probably not needed. Similarly, turbulence generated by wind shifts is probably not a factor in molecular losses in this turbulent inlet.;

Response: We agree with the reviewer. The Reynolds number inside the inlet was about 15000. However, according to our laboratory tests we found that the instrument response increased substantially as the inlet flow rate increased with respect to a constant GSA concentration. To clarify the reviewer's question, we have revised paragraph 2 in section 3.1 as following:

GSA is highly sticky to almost all kind of surfaces. In order to minimize the inlet losses, a short inlet and a high sampling flow rate are used for the GSA measurement, with a similar working principle as a fast-flow reactor (Seeley et al., 1993). The inlet is a 60 cm long 10 cm ID aluminum tube, allowing about 1200 slpm sample flow. The sample residence time is about 0.2 s. Meanwhile, the fast flow rate induces a high Reynolds number turbulent flow with an eddy scale near the diameter of the inlet. Consequently, the small eddies induced by the surface friction are suppressed by the large eddies dominated by the inertial force. GSA sample at the center of the flow must penetrate the small eddies at the edge before colliding with the inlet surface. Hence, inlet losses can be minimized. This is consistent with our ambient test results, showing that the instrument response increases with a higher flow rate with respect to a constant GSA concentration. However, wind gust with a speed of a few m s-1 may still impact the inlet flow pattern, especially when the wind direction is perpendicular to the inlet. Figure 2 presents (a) a polar plot of the NSD with wind direction (North = 0 degree) and (b) a scatter plot of NDS with wind direction. Overall, NSD scatters in all wind direction with a slight bias under NW wind, but NSD is symmetrically distributed at any wind speed. This result is explained by the orientation of the inlet, i.e., when wind blows from perpendicular to the inlet or at a higher speed, more wall loss is expected as the

air flow changes direction for both cases, but this bias is statistically insignificant.

5) p. 5028, line 19. The authors state that cleaner conditions lead to higher gaseous sulfuric acid (GSA) concentrations due to the reduction of aerosol surface. But is there also not a substantial decrease in SO2 from the clean air direction? This would be a good location to look independently at the production and loss terms and see which is driving the increase in GSA abundance in cleaner conditions.

Response: Figure 5 shows a typical transition process from a clean day (23 August) to relative polluted days (24 and 25 August). GSA calculated from Eq. (2) matches very well with GSA observations except on 23 August (a nucleation day), indicating that GSA is primarily generated from OH + SO2 reactions and transferred into the aerosol phase through either nucleation or condensation onto existing aerosol surfaces. The simulated high GSA concentration on August 23 is mainly the result of low aerosol surface area, since all air pollutants are low at the same time.

6) p. 5029, lines 1-5. The authors attribute the increase in GSA concentrations during the pollution control period to those mitigation efforts. However, since GSA is heavily controlled by OH production, might seasonal variations in actinic flux (due to cloudiness, for example), or changes in meteorology (more flow from the northwest) or humidity be equally likely to cause these changes? This is another opportunity to look at the elements in the production and loss terms to see what is really controlling GSA concentrations in this time period relative to the before- and after-control period.

Response: Compared to the period prior to 8 August, at the PKU site daytime (6 a.m. to 6 p.m.) average SO2 increased from 3.7 to 4.5 ppbv while aerosol surface area decreased from 1000 to 570 μm2 cm-3 during the Olympic Games period (8-23 August). Meanwhile, the calculated OH concentration increased from 0.4 $\times$ 10ˆ6 to 1.9 $\times$ 10ˆ6 molecules cm-3. The unexpected increase in SO2 was probably due to the fact that SO2 in Beijing was controlled by some regional sources. Since GSA production can be enhanced by stronger actinic flux and uptake by preexisting aerosol surfaces repre-

sents the dominant sink for GSA, an increasing trend in the daily GSA concentration is evident in Fig. 3, especially during the Olympics and Paralympics period, when more stringent air quality control measures were adopted. Consequently, the frequency of the peak H2SO4 concentration exceeding 5 $\times$ 10ˆ6 molecule cm-3 increases by 16% during August 8-23, compared to the time period prior to August 8. This trend is consistent with that of the frequency of new particle formation events (Yue et al., 2010).

7) In figures 4 and 5, some of the plotted parameters are not scaled to zero, but are expanded to zoom in on the variability. I believe this is misleading, as it emphasizes very small perturbations that may not really be associated with GSA. For example, in Fig. 5, sulfate production rates from GSA are scaled from 0 to 0.014 ug/m3/hr. The co-plotted Aitken-mode sulfate scale goes from 1.6 to 2.1 ug/m3. The change in Aitken mode sulfate mass that is purported to be associated with the GSA diurnal cycle is about 0.35 ug/m3, or about 20% of the total Aitken sulfate mass. If this axis were plotted from 0 to 2.1 ug/m3, it would be evident that the GSA maximum is largely uncorrelated with Aitken mode sulfate mass. The zoomed-in axis artificially emphasizes a very small perturbation to the sulfate budget. Furthermore, it would take more than 2 days of peak production of GSA to account for this âĹij20% perturbation to the Aitken mode sulfate budget. It is evident that parameters other than instantaneous production of GSA control the sulfate mass. This lack of quantitative correspondence is not discussed, and is in fact masked by the chosen scale of the ordinate. This graph scaling, and the lack of discussion of the relevance of the observed GSA to the sulfate budget, must be corrected in a revised manuscript.

Response: The scales of Figs. 6a and 6b have been expanded to a similar scale as the sulfates. We have revised the discussion on sulfate formation as following:

The typical GSA to aerosol sulfate conversion process can be demonstrated by Fig. 5, which displays the GSA time series from 23 to 25 August, i.e., a nucleation day followed by two relatively polluted days. The calculated GSA trace matches the observation very well except on 23 August, since nucleation is not accounted for in Eq. (2). The sim-

ulated high GSA concentration on August 23 is the result of low aerosol surface area, since all air pollutants appears to be low at the same time. Therefore, we believe that GSA is primarily generated from OH + SO2 reactions and transferred into the aerosol phase through either nucleation or condensation onto existing aerosol surfaces. Since SO2 in Beijing is controlled by regional sources and aerosol sulfate can be suspended in the air for several days, the sulfate measured at the PKU site typically has an oxidation history that cannot be explained by local GSA measurements. As shown in Fig. 6c, the PM1 sulfate to SO2 ratio significantly reduces the diurnal variation of sulfate, indicating that most aerosol sulfate has been formed before arriving at the PKU site. Therefore, it is reasonable to use the hour-average of the whole data set to investigate the correlation between the aerosol sulfate and GSA. Assuming the same GSA production rate from the source region to the PKU site, we obtain an average of 0.6 μg m-3 per day sulfate production from the GSA condensation. Given that PM1.0 sulfate has a daily average concentration of about 17 μg m-3 and a residence time of 3 to 7 days, GSA condensation can contribute to 10 – 25% of PM1 sulfate. Moreover, the slight decreasing trend in Fig. 6c indicates that air mass with less sulfate but more SO2 is mixed down, which makes sulfate productions through cloud processing less likely.

8) p. 5030, lines 19-20. Continuing on point (7) above, it is extremely unlikely that intermodal coagulation can explain the very large amount of sulfate in the accumulation mode. The measured in-situ GSA production rates for both the Aitken and accumulation modes are far too small to source this much sulfate over reasonable time frames. The only logical explanations are a) that GSA production rates are much higher in the source regions, which are primarily industrial areas upwind of Beijing, where SO2 is more concentrated, and/or b) other production mechanisms such as in-cloud oxidation contribute the bulk of the particulate sulfate production. It is likely that the GSA concentrations measured in Beijing have no real correspondence to particulate sulfate concentrations, which are the time-integrated product of oxidation processes occurring over many days since the time of emission. Measurements in the plumes of coal-fired industries indicate conversion of SO2 to sulfate by OH oxidation over e-folding time

scales of 2-3 days, giving plenty of time for production of the sulfate observed in Beijing.

Response: We agree with the reviewer that local GSA condensations can only contribute to a small portion of the PM1 sulfate, i.e., 10 – 25%. However, Fig. 6c indicates that in-cloud processing is not likely to be the other sulfate production mechanism. Therefore, we revised the sentence as following: The high sulfate concentration measured at the PKU site may be a result of accumulated oxidation process, occurring over many days since the time of SO2 emission. Moreover, the GSA productions are likely much higher in the source regions, which are primarily industrial areas with much more concentrated SO2.

9) p. 5030, lines 21-23. I don't understand the logic of this sentence. Why does it follow that other sources of particle mass lead to fine-mode sulfate production in Beijing?

Response: The sentence has been revised as "It has been suggested by Guo et al. (2010) that fine mode sulfate in the Beijing area can mainly arise from secondary sources, since no indications of primary contributions from either biomass burning or automobile exhausts were found."

References:

Guo, S., Hu, M., Wang, Z. B., Slanina, J., and Zhao, Y. L.: Size-resolved aerosol water-soluble ionic compositions in the summer of Beijing: implication of regional secondary formation, Atmos. Chem. Phys., 10, 947-959, 10.5194/acp-10-947-2010, 2010.

Seeley, J. V., Jayne, J. T., and Molina, M. J.: HIGH-PRESSURE FAST-FLOW TECHNIQUE FOR GAS-PHASE KINETICS STUDIES, Int. J. Chem. Kinet., 25, 571-594, 1993.

Zheng, J., Khalizov, A., Wang, L., and Zhang, R.: Atmospheric Pressure-Ion Drift Chemical Ionization Mass Spectrometry for Detection of Trace Gas Species, Anal. Chem., 82, 7302-7308, doi:10.1021/ac101253n, 2010.

Please also note the supplement to this comment:
http://www.atmos-chem-phys-discuss.net/11/C4810/2011/acpd-11-C4810-2011-supplement.pdf

---

Interactive comment on Atmos. Chem. Phys. Discuss., 11, 5019, 2011.

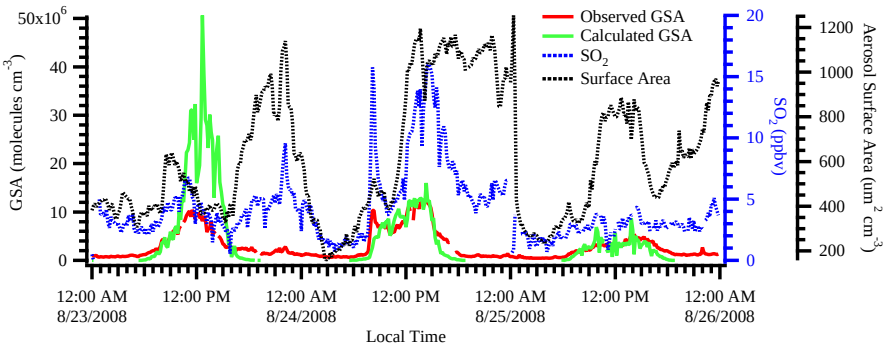

Fig. 1. (Figure 5) Time series of both observed (red) and calculated (green) GSA from 23 to 25 August. Also shown here are the SO2 (blue) and aerosol surface area (black) used in GSA simulation.

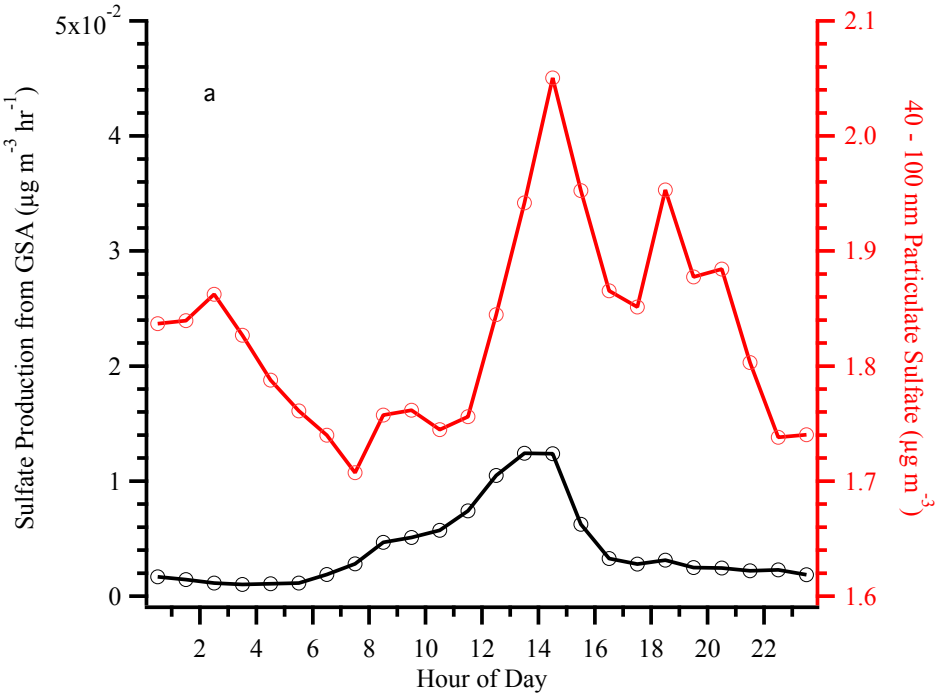

Fig. 2. (Figure 6a) Diurnal profiles of condensation rates of GSA onto Aitken mode aerosols (40-100 nm) and sulfate concentrations in Aitken mode.

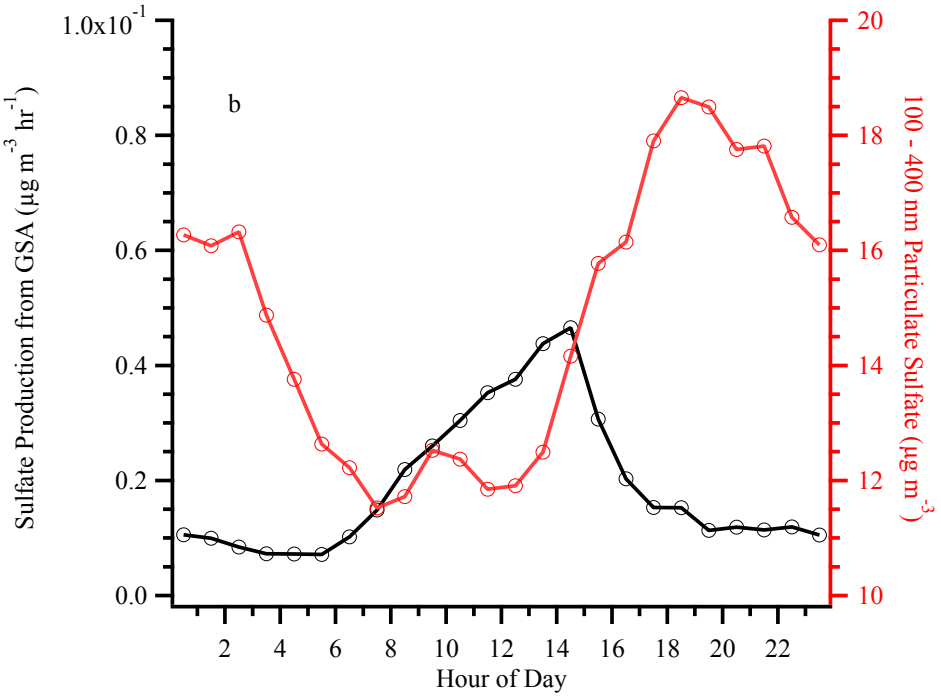

Fig. 3. (Figure 6b) Diurnal profiles of condensation rates of GSA onto accumulation mode particles (100-400 nm) and sulfate concentrations in accumulation mode.

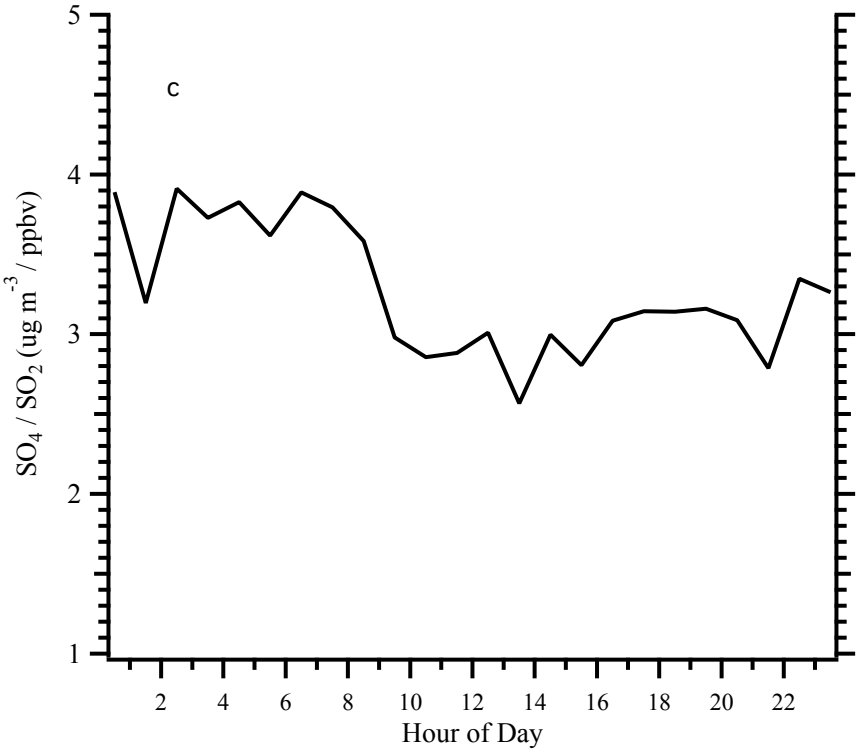

Fig. 4. (Figure 6c) Diurnal profile of PM1 sulfate (SO4) to SO2 ratio.